

# Simulated model of RAPID concept: highlighting innate inflammation and liver regeneration

J. H. Shi<sup>1,2</sup> , X. Yan<sup>1</sup>, S. J. Zhang<sup>1</sup> and P. D. Line<sup>2,3</sup>

<sup>1</sup>Department of Hepatobiliary and Pancreatic Surgery, Henan Key Laboratory of Digestive Organ Transplantation, First Affiliated Hospital of Zhengzhou University, Zhengzhou University, Zhengzhou, China, and <sup>2</sup>Department of Transplantation Medicine, Oslo University Hospital, Rikshospitalet, and <sup>3</sup>Institute of Clinical Medicine, Faculty of Medicine, University of Oslo, Oslo, Norway

Correspondence to: Dr J. H. Shi, Department of Hepatobiliary and Pancreatic Surgery, First Affiliated Hospital of Zhengzhou University, Zhengzhou University, Zhengzhou, China (e-mail: jihuashi@zzu.edu.cn)

**Background:** The resection and partial liver segment II/III transplantation with delayed total hepatectomy (RAPID) concept is a novel transplantation technique for removal of non-resectable liver tumours. The aim of this study was to establish a simulated RAPID model to explore the mechanism involved in the liver regeneration.

**Methods:** A RAPID model was created in rats involving cold ischaemia and reperfusion of the selected future liver remnant (FLR), portal vein ligation, followed by resection of the deportalized lobes in a second step. Histology, liver regeneration and inflammatory markers in RAPID-treated rats were compared with those in controls that underwent 70 per cent hepatectomy with the same FLR size. The effects of interleukin (IL) 6 and macrophage polarization on hepatocyte viability were evaluated in an *in vitro* co-culture system of macrophages and BRL hepatocytes.

**Results:** The survival rate in RAPID and control hepatectomy groups was 100 per cent. The regeneration rate was higher in the RAPID-treated rats, with higher levels of IL-6 and M1 macrophage polarization ( $P < 0.050$ ). BRL hepatocytes co-cultured with M1 macrophages showed a higher proliferation rate through activation of the IL-6/signal transducer and activator of transcription 3/extracellular signal-regulated kinase pathway. This enhancement of proliferation was inhibited by tocilizumab or gadolinium trichloride ( $P < 0.050$ ).

**Conclusion:** The surgical model provides a simulation of RAPID that can be used to study the liver regeneration profile.

## Surgical Relevance

The mechanisms sustaining liver regeneration are a relevant field of research to reduce the 'small for size' liver syndrome when the future liver remnant is not adequate. Several surgical strategies have been introduced both for liver resection and transplant surgery, mostly related to this issue and to the scarcity of grafts, among these the RAPID concept involving the use of an auxiliary

segment II/III donor liver that expands to a sufficient size until a safe second-stage hepatectomy can be performed. Understanding the mechanisms and pitfalls of the liver regeneration profile may help in tailoring surgical strategies and in selecting patients. In this experimental model the authors investigated liver histology, regeneration and inflammatory markers in RAPID-treated rats.

## Funding information

Hepatobiliary Research Foundation of Henan Digestive Disease Association, China, GDZX2019004  
Medical Science and Technology Programme of Henan, China SBGJ2018023

Paper accepted 5 June 2020

Published online 15 July 2020 in Wiley Online Library (www.bjsopen.com). DOI: 10.1002/bjs5.50322

## Introduction

Liver resection is a potential curative treatment option for patients with primary and secondary liver tumours. Most patients are not suitable for resection owing to large tumour load or multiple tumours that cannot be

removed completely because of an insufficient size of the future liver remnant (FLR). The remnant liver needs to be of adequate size and quality to avoid small-for-size liver syndrome with associated high morbidity and mortality rates. Various strategies such as portal vein embolization<sup>1</sup>,

two-stage hepatectomy<sup>2</sup> and associating liver partition and portal vein ligation for staged hepatectomy (ALPPS)<sup>3</sup> have been developed to increase the FLR and enable surgery in patients otherwise deemed to have unresectable disease. Previous studies indicated that the size of the FLR should be at least 25–30 per cent of standard liver volume<sup>4</sup>, or that the ratio between liver graft mass and recipient bodyweight should be above 0.5–0.8 per cent<sup>5,6</sup>.

Liver transplantation is standard of care for selected patients with hepatocellular carcinoma, and high overall survival rates might also be obtained in highly selected patients with non-resectable colorectal liver metastases<sup>7,8</sup>. Scarcity of liver grafts is, however, severely limiting the feasibility of introducing liver transplantation as a treatment for secondary liver tumours. The resection and partial liver segment II/III transplantation with delayed total hepatectomy (RAPID) concept, involving use of an auxiliary segment II + III donor liver that expands to a sufficient size until a safe second-stage hepatectomy can be performed, was recently reported by Line and colleagues<sup>9</sup>. This technique might provide more patients with the option of liver transplantation for non-resectable liver tumours. In the RAPID setting, the size of the transplanted graft relative to standard liver volume and graft mass is far below the minimum graft size for transplantation, and few studies have reported successful results with such a small FLR<sup>10</sup>. However, the exact mechanism of RAPID-associated liver regeneration remains unclear.

Portal vein ligation and transection alone in humans and mice has been shown to trigger the systemic release of interleukin (IL) 6, and comparable intrahepatic expression of F4/80, an M1 macrophage marker, in liver regeneration after ALPPS<sup>11</sup>, indicating that a rapid increase in liver volume might be mediated by systemic release of the pro-inflammatory cytokine after ALPPS. Liver macrophages are well known to release IL-6 for the priming of hepatocyte proliferation in liver regeneration after partial hepatectomy<sup>12,13</sup>. However, the role of macrophages and IL-6 in liver regeneration is still debated because the results of macrophage depletion and IL-6 treatment are controversial. Some studies<sup>14,15</sup> found that macrophage depletion before hepatectomy enhanced liver regeneration after partial hepatectomy, whereas others<sup>16</sup> reported that the regeneration process was inhibited<sup>16</sup>. Inoculation of IL-6 into hepatocytes seemed to result in either stimulation or inhibition of DNA synthesis<sup>17,18</sup>.

To further elucidate the mechanism underlying the post-operative regeneration and functional restoration in a small liver graft, an animal model mimicking the physiological conditions in the RAPID setting was developed to simulate a clinically relevant setting. The primary aim of this study

was to compare the liver regeneration profile between a RAPID protocol and a hepatectomy group that had an identical FLR. The macrophage activation involved in the RAPID-related regenerative process was also evaluated.

## Methods

A total of 33 12-week-old male SD rats (Keli China Experimental Animal Centre, Beijing, China) from Henan Experimental Animal Centre (Zhengzhou, China) were used in all experiments. Rats were allowed free access to chow and water before and after surgical procedures. Experimental protocols were approved by the animal ethics committee of the First Affiliated Hospital of Zhengzhou University (registration number 2019-KY-183), and were carried out according to institutional guidelines in accordance with the ARRIVE guidelines<sup>19</sup>. Bodyweight, survival rate and complications were recorded daily.

## Experimental model

Based on research on rodent liver anatomy for the partial hepatectomy and ALPPS model<sup>20</sup>, a previous model intended to mimic the RAPID procedure was modified, whereby the FLR was subjected to cold ischaemia–reperfusion injury, and the rest of the liver was deportalized before further resection (*Fig. S1*, supporting information). Anaesthesia was induced with a subcutaneous injection of 1:1 fentanyl/midazolam at a dose of 0.15–0.30 ml per 100 g bodyweight<sup>21</sup>. On day 0, the first step (step I) was performed to obtain a suitably small FLR (left lobe, 30 per cent of total liver volume); this comprised parenchymal transection in the median lobe, *in situ* ischaemia of the left lobe for 60 min by clamping both the portal vein and hepatic artery in the left lobe pedicle, and liver preservation at 0–4°C in a plastic bag containing saline and ice, followed by reperfusion by declamping of the left lobe, and ultimately portal vein ligation of the remaining 70 per cent of liver parenchyma. Heparin was administered intravenously at a dose of 300 units/kg 10 min before *in situ* ischaemia of the left lobe. Three days after step I surgery, the animals underwent a second laparotomy to remove the deportalized liver lobes after ligation of the lobar arteries and bile ducts (step II). In the control (hepatectomy) group, a standard 70 per cent hepatectomy was performed, with removal of the median and left lobes, resulting in the same FLR as the RAPID group.

To harvest samples, three rats were killed at each of the following time points in the RAPID group ( $n = 21$ ): before surgery (baseline), on days 1 and 3 after step I surgery, and days 1, 3, 7 and 21 after step II. In the hepatectomy

group ( $n = 12$ ), three animals were killed on days 1, 3, 7 and 21 after partial hepatectomy. The rats killed before surgery (baseline) in the RAPID group were regarded as the sham operative control for each group. Plasma samples were obtained from the infrahepatic vena cava after death to measure the protein levels of IL-6, and liver samples were harvested from the remnant liver to assess parameters of hepatic sinusoidal injury and liver regeneration.

### ***In vivo* liver regeneration**

The FLR weight was recorded after step I and step II surgery. Kinetic growth rate (KGR), describing the percentage increase in remnant liver per day, and the ratio of remnant liver weight relative to bodyweight (LBW) were calculated<sup>20</sup>. Formalin-fixed and frozen liver tissue specimens were stained with haematoxylin and eosin, and immunostained for assessment of hepatocyte proliferation. Proliferation was further evaluated by assessment of Ki-67 using immunohistochemistry (IHC), and proliferating cell nuclear antigen (PCNA) by means of western blotting<sup>20</sup>.

### **Isolation of bone marrow-derived macrophages and macrophage polarization assay**

Bone marrow-derived macrophages (BMDMs) were prepared as described previously<sup>22</sup>, from the femurs and tibias of naive control rats. BMDMs were cultured in L929 conditioned medium (Shanghai Cell Bank, Chinese Academy of Sciences, Shanghai, China) for 7 days and allowed to differentiate into mature macrophages (M0). Polarization of BMDMs to M1 macrophages was induced by treatment with lipopolysaccharide (100 ng/ml; Sigma Aldrich, St Louis, Missouri, USA) for 24 h before further biochemical analysis. Immunofluorescence and IHC were performed to detect expression levels of the M1-related marker CD68, and inducible nitric oxide synthase (iNOS), related to macrophage polarization from *in vitro* culture and tissue slices.

### **Co-culture of hepatocytes with bone marrow-derived macrophages and cell proliferation assay**

Rat hepatocytes, BRL (Shanghai Cell Bank), were co-cultured with the conditioned medium from induced rat macrophages, in the following treatment groups: control (BRL cells without any treatment); BRL + M0 (BRL cells co-cultured with conditioned medium from non-polarized macrophages); BRL + M1 (BRL cells co-cultured with conditioned medium from M1 macrophages);

BRL + M1 + anti-IL-6 (BRL cells co-cultured with conditioned medium from M1 macrophages and anti-IL-6); and BRL + antimacrophage-treated M1 macrophages (BRL cells co-cultured with conditioned medium from antimacrophage-treated M1 macrophages).

BRL cells were treated with the IL-6 receptor inhibitor tocilizumab<sup>23</sup> (0.5 mg/ml; Roche, Basle, Switzerland) 1 h before addition of conditioned medium from M1 macrophages. For depletion of M1, BRL cells were cultured with conditioned medium from M1 macrophages that had been treated with the macrophage inhibitor gadolinium trichloride<sup>24</sup> (100  $\mu$ mol/l; Sigma-Aldrich).

The viability of co-cultured BRL cells was determined using 3-(4,5-dimethyl-2-thiazolyl)-2,5-diphenyl-2-H-tetrazolium bromide (MTT) at 24 and 48 h after stimulation with 10 nmol/l epidermal growth factor (EGF; E-1257; Sigma-Aldrich)<sup>25</sup>.

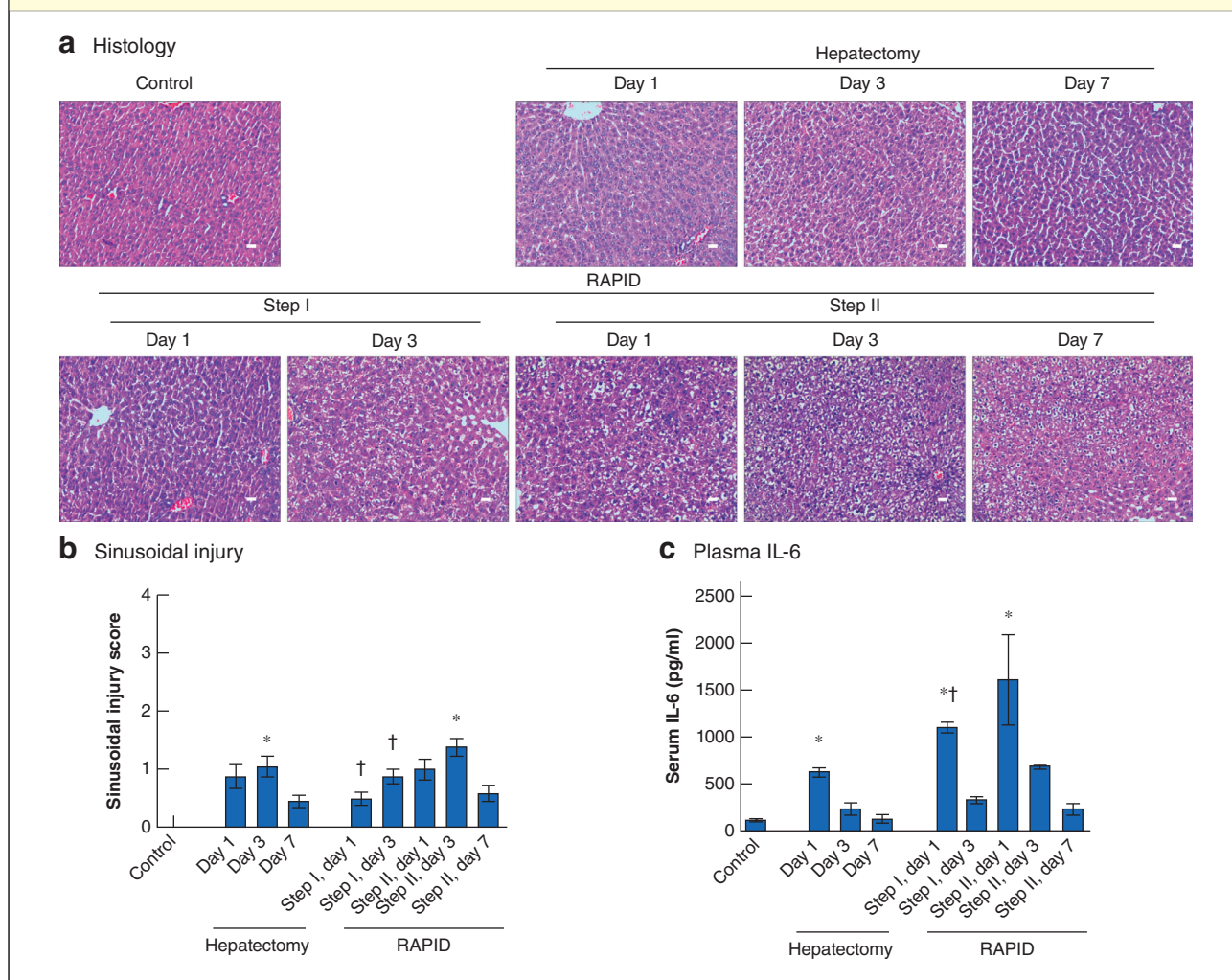
### **Immunohistochemical assessment**

Formalin-fixed and paraffin-embedded liver tissue specimens were stained with haematoxylin and eosin, and immunostained using antibodies against Ki-67 (1:200; Abcam, Cambridge, UK), macrophage-related marker CD68 (1:200; Chemicon International, Temecula, California, USA), M1-related marker iNOS (1:100; Santa Cruz Biotechnology, Santa Cruz, California, USA) and M2-related marker CD163 (1:500; Abcam), as described previously<sup>20</sup>. The histological analyses were performed in a blinded fashion and the number of positive cells was determined in five random visual fields (original magnification  $\times 200$ ) per section using a Nikon ECLIPSE Ni-E400 microscope and NIS Elements Basic Research Microscope Imaging Software (Nikon, Tokyo, Japan).

### **Western blotting**

A standard western blot assay was used to analyse protein expression, using primary antibodies against signal transducer and activator of transcription 3 (STAT3) (1:1000; Cell Signaling Technology, Beverly, Massachusetts, USA), phosphorylated STAT3 (1:1000; Cell Signaling Technology), extracellular signal-regulated kinase (ERK) 1 (1:1000; Santa Cruz Biotechnology, Santa Cruz, USA), phosphorylated ERK (1:2000; Cell Signaling Technology), PCNA (1:1000; Cell Signaling Technology) and  $\beta$ -tubulin (1:5000; Sigma Aldrich), as described previously<sup>20</sup>. The immunoreactive signals were visualized by scanning densitometry with the ChemiDoc™ Touch Imaging System (Bio-Rad Laboratories, Hercules, California, USA).

**Fig. 1 Typical microscopic changes, quantification of sinusoidal injury and plasma interleukin 6 levels after 70 per cent hepatectomy and RAPID procedure**



**a** Histology (haematoxylin and eosin staining, original magnification  $\times 200$ , scale bars 50  $\mu\text{m}$ ); **b** sinusoidal injury scores, on a scale from 0 to 4; and **c** plasma interleukin (IL) 6 levels. Values are mean(s.d.) ( $n = 3$  per group). \* $P < 0.050$  versus day 0 (control) (ANOVA); † $P < 0.050$  versus same time point in hepatectomy group (Student's  $t$  test).

### Enzyme-linked immunosorbent assay

Plasma levels of the proinflammatory cytokine IL-6 were determined using commercially available enzyme-linked immunosorbent assays (Solarbio, Beijing, China) according to the manufacturer's instructions<sup>21</sup>.

### Statistical analysis

Values are reported as mean(s.d.), unless stated otherwise. Differences were analysed using ANOVA (among time points) and Student's  $t$  test (between RAPID and hepatectomy groups), with  $F$  and  $t$  values calculated respectively. A probability level of less than 5 per cent was

considered statistically significant. SPSS<sup>®</sup> version 21.0 (IBM, Armonk, New York, USA) was used for statistical analysis.

### Results

All the animals tolerated the surgical procedures well. The survival rate after surgery was 100 per cent, with no significant morbidity.

### Histology

Histological analysis of the remnant liver revealed hepatic sinusoidal injury and hepatocyte mitosis. The sinusoidal

injury was characterized by sinusoidal inflammation in the periportal area, sinusoidal dilatation and microvesicular steatosis (Fig. 1a)<sup>20</sup>. These microscopic changes, evaluated using the sinusoidal injury score, were most prominent on days 1 and 3 after operation in the hepatectomy group (day 3:  $F = 3.360$ ,  $P = 0.044$ ), and on days 1 and 3 after step II surgery in the RAPID group (day 3:  $F = 8.367$ ,  $P = 0.001$ ). The sinusoidal injury within 3 days after step I surgery in the RAPID group was notably different from that in the hepatectomy group ( $t = 3.055$ ,  $P = 0.018$  on day 1;  $t = 6.000$ ,  $P = 0.001$  on day 3) (Fig. 1b).

### Inflammatory markers

Plasma levels of IL-6 are shown in Fig. 1c. The levels of IL-6 increased in response to surgery in both groups on day 1 and were still raised on day 3 (day 1:  $F = 23.233$ ,  $P = 0.001$  and  $F = 6.717$ ,  $P = 0.007$  in hepatectomy and RAPID groups respectively). In RAPID-treated animals, the IL-6 level on day 1 after step I surgery was significantly higher than that in the hepatectomy group on day 1 ( $t = 6.203$ ,  $P = 0.003$ ). There was a further substantial increase in IL-6 level by day 1 after step II surgery ( $F = 6.405$ ,  $P = 0.003$ ), and this was raised compared with the level in the hepatectomy group.

Expression of proteins characteristic of the proinflammatory macrophage (M1) phenotype, CD68 and iNOS, in the regenerating liver is shown in Fig. 2. In the hepatectomy group, the staining of CD68 and iNOS was most prominent on days 1 and 3 (day 1:  $F = 28.385$ ,  $P = 0.001$  and  $F = 34.562$ ,  $P = 0.001$  respectively), whereas in the RAPID group the strongest expression was observed on days 1 and 3 after step II surgery (day 1:  $F = 10.629$ ,  $P = 0.001$  and  $F = 11.704$ ,  $P = 0.001$ ). The maximum intrahepatic expression of CD68 and iNOS was comparable on day 1 after RAPID step II surgery and day 1 after hepatectomy (both  $t = 0.707$ ,  $P = 0.519$ ); RAPID treatment triggered sustained activation of M1 macrophages following the two steps of surgery. Expression of CD68 and iNOS on day 1 after step I surgery was significantly lower than that 1 day after hepatectomy alone ( $t = 4.000$ ,  $P = 0.016$  and  $t = 4.111$ ,  $P = 0.015$  respectively). CD68 and iNOS were initially localized in the periportal zone (zone I), which was highlighted on day 1 after hepatectomy, and gradually moved to the pericentral zone (zone II and III) of the liver acinus. The distribution of anti-inflammatory (M2) macrophages visualized by CD163 staining was not significantly changed (data not shown).

### RAPID-induced liver regeneration profile

The magnitude of liver regeneration following the surgical interventions was first evaluated by assessment of

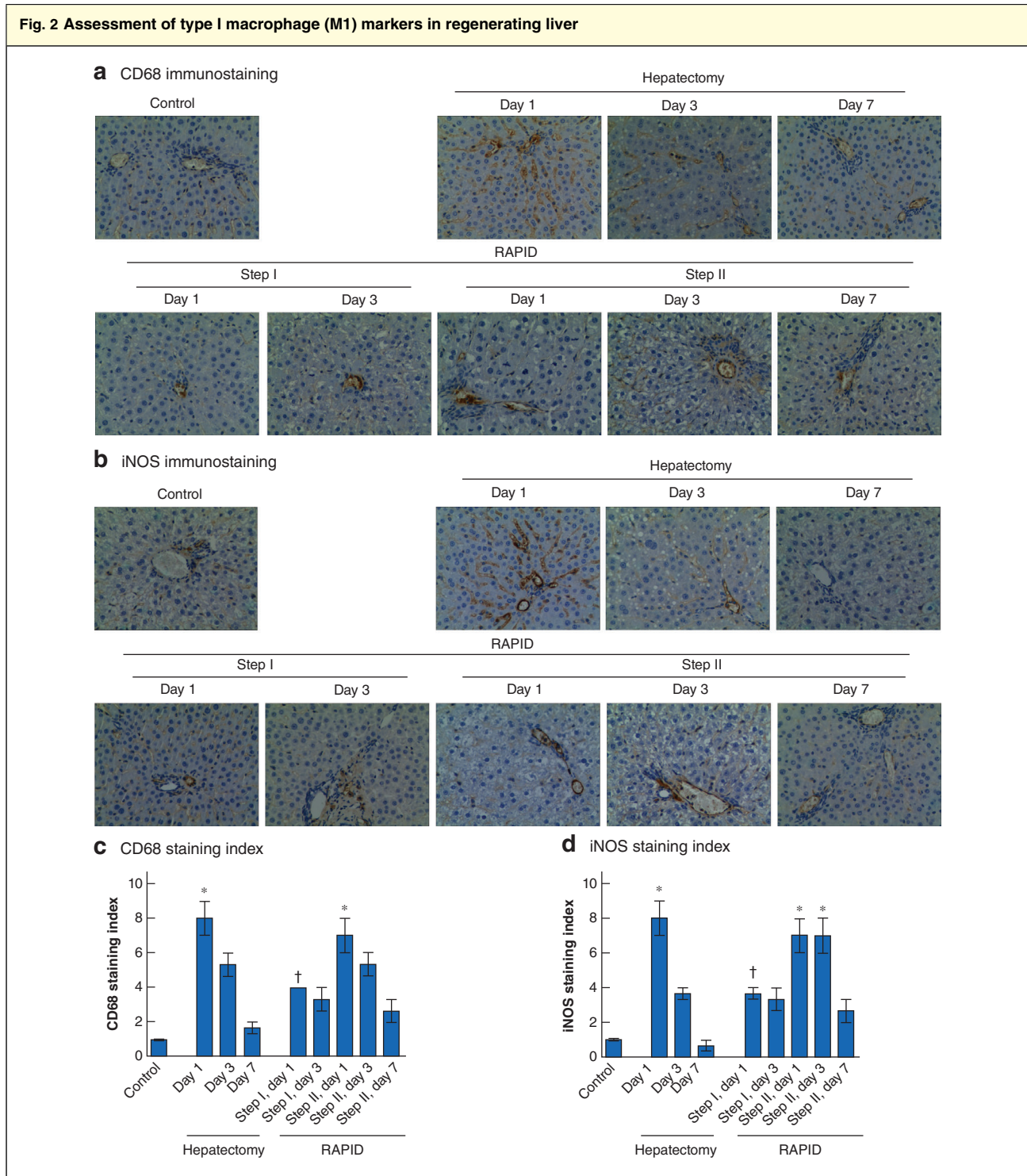
the KGR and LBW ratio. Dynamic changes in the FLR weight with time in the RAPID group correlated with KGR (Fig. 3a). In the RAPID group, mean(s.d.) KGR between days 0 and 1 ( $KGR_{I0-1}$ ) and days 1 and 3 after step I surgery was 45.4(10.1) and 36.1(5.7), and that between days 0 and 1, days 1 and 3, days 3 and 7, and days 7 and 21 after step II surgery was 12.5(2.8), 1.6(1.1), 1.7(1.9) and 1.6(1.2) per cent/day, respectively. In the hepatectomy group, the mean KGR between days 0 and 1 ( $KGR_{0-1}$ ), days 1 and 3, days 3 and 7, and days 7 and 21 was 33.8(8.6), 36.5(4.2), 7.2(2.5) and 0.5(0.5) per cent/day. Mean  $KGR_{I0-1}$  in the RAPID group was higher than  $KGR_{0-1}$  in the hepatectomy group but the difference did not reach statistical significance ( $t = 1.706$ ,  $P = 0.163$ ).

The LBW ratio in the RAPID group on day 1 after step II surgery was not significantly different from that 7 days after hepatectomy ( $t = 0.069$ ,  $P = 0.948$ ), indicating that it took 4 days to restore the complete liver mass in the RAPID group whereas it took 7 days to restore the original liver size after hepatectomy. To further compare the regeneration profile in the two groups, Ki-67 and PCNA were evaluated in tissue samples of the FLR by IHC and western blot respectively. Ki-67 and PCNA expression were maximal within 3 days after step I surgery ( $F = 20.941$ ,  $P = 0.001$  and  $F = 81.563$ ,  $P = 0.001$  respectively). Expression of Ki-67 and PCNA on day 1 after RAPID step I surgery was significantly higher than that 1 day after hepatectomy ( $t = 10.126$ ,  $P = 0.001$  and  $t = 8.506$ ,  $P = 0.001$ ) (Fig. 3).

### M1 macrophage polarization and interleukin 6-STAT3-ERK signalling pathway

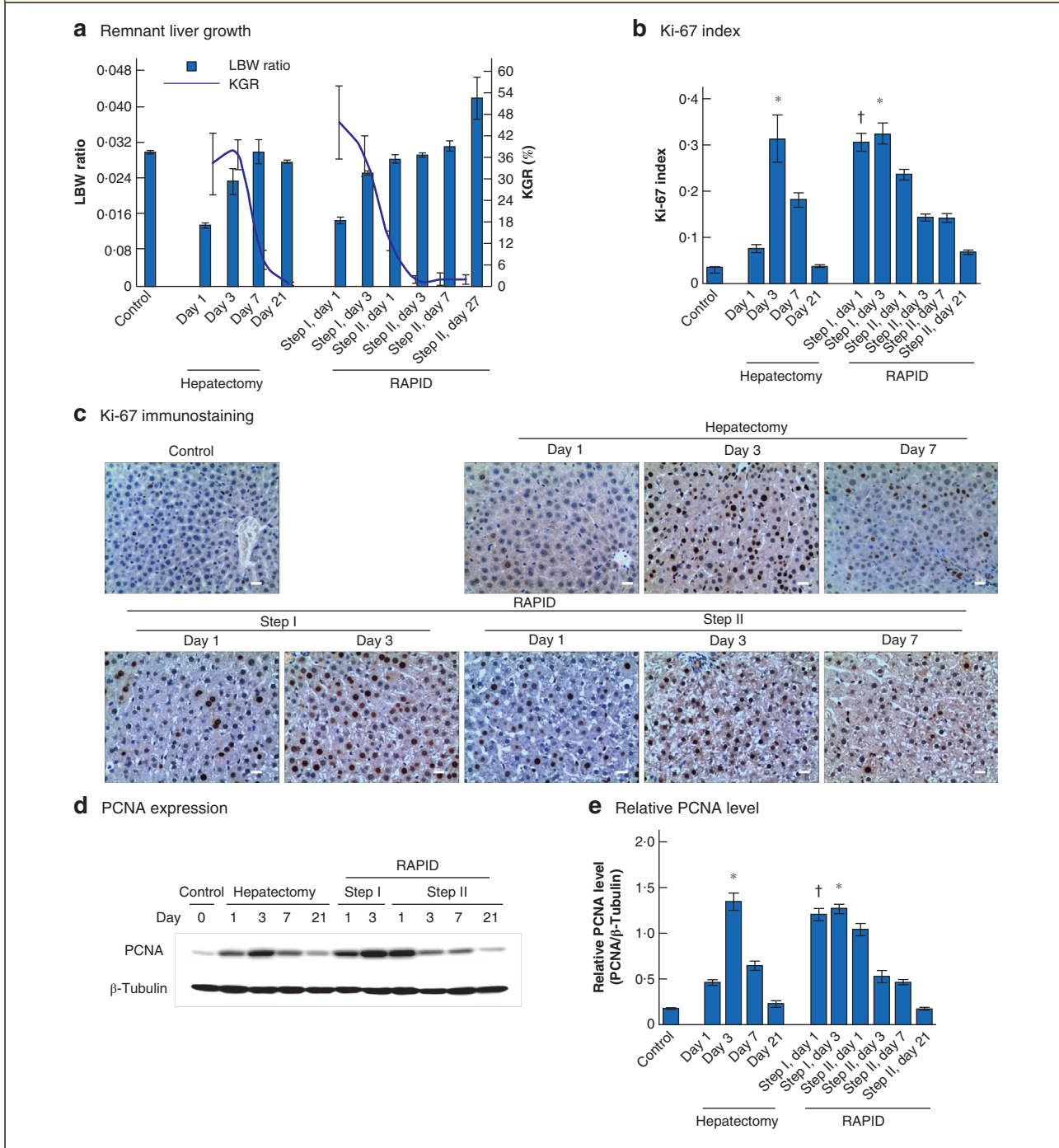
At 24 and 48 h after stimulation with EGF, BRL hepatocytes co-cultured with conditioned medium from M1 macrophages showed increased cell viability compared with hepatocytes cultured with M0 medium and untransformed hepatocytes ( $F = 4.081$ ,  $P = 0.026$  and  $F = 3.030$ ,  $P = 0.043$  at 24 and 48 h respectively). Cell viability was lower when the BRL hepatocytes were co-cultured with medium pretreated with anti-IL-6 (tocilizumab) or anti-M1 macrophage (gadolinium trichloride) (24 h:  $t = 2.160$ ,  $P = 0.042$  and  $t = 2.088$ ,  $P = 0.049$  respectively; 48 h:  $t = 2.205$ ,  $P = 0.025$  and  $t = 2.411$ ,  $P = 0.038$  respectively) (Fig. 4a).

*In vitro* co-culture of BRL hepatocytes with M1 showed that M1 activated signalling pathways of STAT3 and ERK by 30 min after EGF stimulation. PCNA was upregulated at 24 h. Activation of both STAT3 and ERK, and

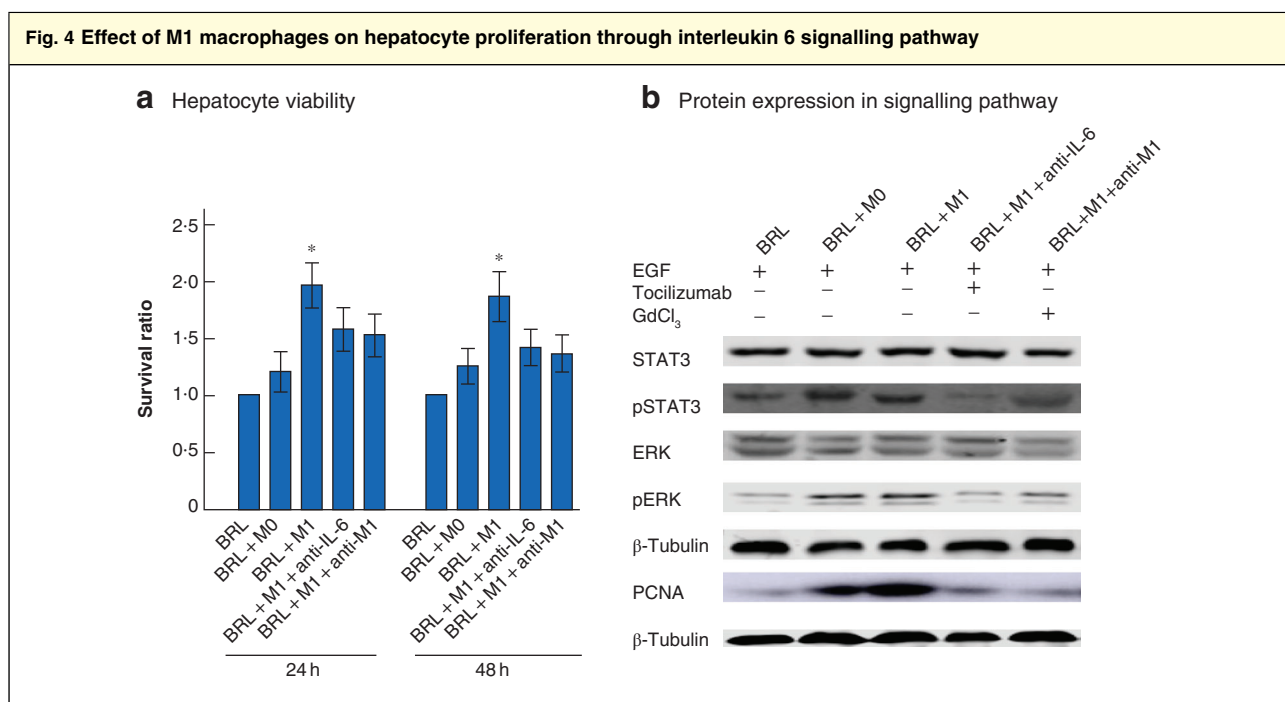


Examples of immunostaining of **a** CD68 and **b** inducible nitric oxide synthase (iNOS) in control, after 70 per cent hepatectomy, and after steps I and II of the simulated RAPID procedure (haematoxylin counterstain, original magnification  $\times 200$ ). Semiquantification of **c** CD68 and **d** iNOS immunostaining. Values are mean(s.d.) ( $n = 3$  per group). \* $P < 0.050$  versus day 0 (control) (ANOVA); † $P < 0.050$  versus same time point in hepatectomy group (Student's *t* test).

**Fig. 3 Evaluation of liver regeneration after surgical interventions**



**a** Time course of ratio of future liver remnant to bodyweight (LBW) and kinetic growth rate (KGR) of the remnant liver after 70 per cent hepatectomy and simulated RAPID procedure. **b** Semiquantitative evaluation of Ki-67 proliferation index and **c** examples of Ki-67 immunostaining (haematoxylin counterstain, original magnification  $\times 200$ , scale bars 50  $\mu\text{m}$ ). **d** Western blot showing proliferating cell nuclear antigen (PCNA) protein expression and **e** quantitative analysis of PCNA relative to  $\beta$ -tubulin expression. Values are mean (s.d.) ( $n = 3$  per group). \* $P < 0.050$  versus day 0 (control) (ANOVA); † $P < 0.050$  versus same time point in hepatectomy group (Student's  $t$  test).



**a** Viability of BRL hepatocytes co-cultured with non-polarized (M0) macrophages, or M1 macrophages stimulated with epidermal growth factor (EGF) for 24 or 48 h, measured using 3-(4,5-dimethyl-2-thiazolyl)-2,5-diphenyl-2-H-tetrazolium bromide assay, and effect of inhibition of interleukin (IL) 6 with tocilizumab or M1 with gadolinium trichloride (GdCl<sub>3</sub>). Values are mean(s.d.) ( $n = 3$  per group). \* $P < 0.050$  versus BRL and BRL + M0 (ANOVA),  $P < 0.050$  versus BRL + M1 + anti-IL-6 and BRL + M1 + anti-M1 (Student's  $t$  test) at same time point. **b** Western blots showing expression of signal transducer and activator of transcription 3 (STAT3), phosphorylated STAT3 (pSTAT3), extracellular signal-regulated kinase (ERK), phosphorylated ERK (pERK), proliferating cell nuclear antigen (PCNA) and  $\beta$ -tubulin in each BRL hepatocyte treatment group. STAT3 and ERK were activated at 30 min after stimulation with EGF, and PCNA was evaluated at 24 h after stimulation with EGF.

PCNA upregulation were inhibited by either tocilizumab or gadolinium trichloride (Fig. 4b).

## Discussion

The delicate RAPID process comprises auxiliary partial liver transplantation and two-stage hepatectomy, relying on fast liver regeneration in the small graft with avoidance of small-for-size syndrome by portal inflow modulation. A simplified animal model with good reproducibility is needed to clarify the physiological processes involved. As this complex process requires specialized surgical skills, it is difficult to realize with an ideal research model.

Based on a previous ALPPS model, a FLR volume of 20–30 per cent appears to be a safe and reliable model for investigation of liver regeneration in small liver remnants<sup>20</sup>. The simulated RAPID model described here was designed to mimic the RAPID procedure. The overall good tolerability was in line with the previous result of an experimental ALPPS study with a FLR size of 30 per cent<sup>20</sup> and clinical experience reported after the RAPID

procedure<sup>9</sup>. To avoid the complexity of performing an auxiliary partial liver transplantation, the transplant step was replaced by 60 min of cold preservation of the FLR with subsequent reperfusion in the animal model. As the RAPID procedure also entails partial liver resection to make space for an auxiliary graft, parenchymal transection of the median lobe was performed. After reperfusion of the remnant liver, the portal veins of the remaining liver segments were ligated. Although the model does not actually involve transplantation of a small segment, the main physiological (cold ischaemia–reperfusion injury and surgical stress) and anatomical alterations following a RAPID operation are similar. In addition, for practical reasons, it was not possible to obtain reliable measurements of portal pressure in conjunction with the surgical interventions in the two rodent groups. In the clinic, liver volumetry on CT and functional parameters are used mostly to assess liver regeneration kinetics, which may not be feasible in animal laboratories. Biological markers (Ki-67 and PCNA) may provide more precise information on

proliferation and have been used in the most experimental studies<sup>11,20</sup>.

An exceptional regenerative capacity of the liver remnant was demonstrated using the simulation model. The level of hepatic sinusoidal injury was moderate, and less pronounced after RAPID than after 70 per cent hepatectomy. It is still not clear why the RAPID-treated segment, which was subjected to cold ischaemia–reperfusion injury and the stress of parenchymal transection and portal vein ligation, showed less sinusoidal injury in the FLR after step I surgery compared with that after simple 70 per cent hepatectomy. The well preserved liver architecture and sustained stronger regeneration of the small remnant liver after the RAPID step I surgery enabled safe resection of the deportalized liver in step II.

It is well established that IL-6 acts as a complete mitogen during the initiation of hepatocyte proliferation<sup>12</sup>. Furthermore, liver macrophages can act as primer for liver regeneration after partial hepatectomy<sup>13</sup>. However, the role of either macrophages or IL-6 in liver regeneration is still controversial owing to the diverse results from *in vivo* and *in vitro* depletion experiments<sup>14–18</sup>. A study<sup>11</sup> of a mouse ALPPS model demonstrated that the enhanced liver regeneration was associated with systemic release of the inflammatory cytokines IL-6 and tumour necrosis factor  $\alpha$ , but the maximal intrahepatic expression of the M1 macrophage marker F4/80 after ALPPS was comparable to that observed after portal vein ligation or liver transection alone.

In the present study, both *in vivo* and *in vitro* results suggested that M1 macrophage polarization is involved in the accelerated regenerative ability of the remnant liver through upregulation of the IL-6 signal pathway. The levels of IL-6 were higher and sustained over a longer period in the RAPID group. Furthermore, there was a sustained and stronger activation of M1 macrophages visualized by CD68 and iNOS immunostaining. This proinflammatory profile might be related to the combined effect of multiple surgical traumas, such as cold ischaemia and reperfusion injury, parenchymal transection and portal vein ligation, in the RAPID group. To verify whether IL-6 and M1 macrophage polarization influences hepatocyte proliferation, an *in vitro* co-culture experiment was conducted. Hepatocytes co-cultured with M1 macrophages and stimulated via EGF pathways showed a higher hepatocyte proliferation rate and viability. These effects were reversed by inhibition of M1 macrophages or IL-6, suggesting that the findings of the *in vivo* model are important for the magnitude of regeneration in the RAPID setting. This is in line with other model studies of ALPPS and two-stage hepatectomy that suggested a decisive regulatory

role for M1 macrophages that enhance cell proliferation through the synergistic effect of IL-6 in the regenerative process<sup>11,26,27</sup>.

Macrophages play a crucial role in both hepatic injury and liver regeneration through innate inflammatory cytokines<sup>13</sup>. However, the functional role of their activated phenotype (M1/M2) in liver regeneration remains uncertain<sup>28,29</sup>. As regards the effect of IL-6 on liver regeneration, IL-6 may induce liver regeneration and reduce hepatic ischaemia–reperfusion injury<sup>30</sup>. Furthermore, IL-6 as a proinflammatory cytokine mirrors the severity of hepatic injury; a decreased IL-6 level at an early phase after partial liver transplantation was associated with decreased sinusoidal injury and improved animal survival<sup>31</sup>. The present study investigated the relationship between M1 macrophage polarization and liver regeneration, and the results indicated that M1 polarization benefits hepatocyte proliferation through IL-6. During the priming phase of regeneration, IL-6 is an important proinflammatory (M1-type) cytokine, activating immediate-to-early gene expression in hepatocytes through STAT3<sup>32</sup>, and thus promoted hepatocyte proliferation in the present co-culture system. Whether exogenous IL-6 administration and specific introduction of M1 macrophages would promote postoperative liver regeneration in small-for-size liver remnants after RAPID needs further investigation. The regulatory mechanisms of RAPID-related liver injury and regeneration are being investigated in a clinical study<sup>9</sup>, and the model described here may be suitable for testing the major research findings before clinical translation.

## Acknowledgements

The authors thank H.-W. Tang (Henan Key Laboratory of Digestive Organ Transplantation, First Affiliated Hospital of Zhengzhou University, Zhengzhou, China) for technical assistance, and F. Wang (Department of Pathology, First Affiliated Hospital of Zhengzhou University, Zhengzhou, China) for the pathological evaluation. The research study was supported by the Medical Science and Technology Programme of Henan, China (SBGJ2018023), and the Hepatobiliary Research Foundation of Henan Digestive Disease Association, China (GDXZ2019004).

*Disclosure:* The authors declare no conflict of interest.

## References

- 1 Makuuchi M, Thai BL, Takayasu K, Takayama T, Kosuge T, Gunvén P *et al.* Preoperative portal embolization to increase safety of major hepatectomy for hilar bile duct

- carcinoma: a preliminary report. *Surgery* 1990; **107**: 521–527.
- 2 Adam R, Laurent A, Azoulay D, Castaing D, Bismuth H. Two-stage hepatectomy: a planned strategy to treat irresectable liver tumors. *Ann Surg* 2000; **232**: 777–785.
  - 3 Schnitzbauer AA, Lang SA, Goessmann H, Nadalin S, Baumgart J, Farkas SA *et al*. Right portal vein ligation combined with *in situ* splitting induces rapid left lateral liver lobe hypertrophy enabling 2-staged extended right hepatic resection in small-for-size settings. *Ann Surg* 2012; **255**: 405–414.
  - 4 Vauthey JN, Chaoui A, Do KA, Bilimoria MM, Fenstermacher MJ, Charnsangavej C *et al*. Standardized measurement of the future liver remnant prior to extended liver resection: methodology and clinical associations. *Surgery* 2000; **127**: 512–519.
  - 5 Truant S, Oberlin O, Sergent G, Lebuffe G, Gambiez L, Ernst O *et al*. Remnant liver volume to body weight ratio > or =0.5%: a new cut-off to estimate postoperative risks after extended resection in noncirrhotic liver. *J Am Coll Surg* 2007; **204**: 22–33.
  - 6 Breitenstein S, Apestegui C, Petrowsky H, Clavien PA. ‘State of the art’ in liver resection and living donor liver transplantation: a worldwide survey of 100 liver centers. *World J Surg* 2009; **33**: 797–803.
  - 7 Hagness M, Foss A, Line PD, Scholz T, Jørgensen PF, Fosby B *et al*. Liver transplantation for nonresectable liver metastases from colorectal cancer. *Ann Surg* 2013; **257**: 800–806.
  - 8 Dueland S, Line PD, Hagness M, Foss A, Andersen MH. Long-term quality of life after liver transplantation for non-resectable colorectal metastases confined to the liver. *BJS Open* 2018; **3**: 180–185.
  - 9 Line PD, Hagness M, Berstad AE, Foss A, Dueland S. A novel concept for partial liver transplantation in nonresectable colorectal liver metastases: the RAPID concept. *Ann Surg* 2015; **262**: e5–e9.
  - 10 Feng AC, Liao CY, Fan HL, Chen TW, Hsieh CB. A successful child-to-adult deceased donor liver transplantation: a case report and literature review. *Ann Transplant* 2015; **20**: 21–24.
  - 11 Schlegel A, Lesurtel M, Melloul E, Limani P, Tschuor C, Graf R *et al*. ALPPS: from human to mice highlighting accelerated and novel mechanisms of liver regeneration. *Ann Surg* 2014; **260**: 839–846.
  - 12 Zimmers TA, McKillop IH, Pierce RH, Yoo JY, Koniaris LG. Massive liver growth in mice induced by systemic interleukin 6 administration. *Hepatology* 2003; **38**: 326–334.
  - 13 Fausto N, Campbell JS, Riehle KJ. Liver regeneration. *Hepatology* 2006; **43**(Suppl 1): S45–S53.
  - 14 Boulton RA, Alison MR, Golding M, Selden C, Hodgson HJ. Augmentation of the early phase of liver regeneration after 70% partial hepatectomy in rats following selective Kupffer cell depletion. *J Hepatol* 1998; **29**: 271–280.
  - 15 Kandilis AN, Koskinas J, Tiniakos DG, Nikiteas N, Perrea DN. Liver regeneration: focus on cell types and topographic differences. *Eur Surg Res* 2010; **44**: 1–12.
  - 16 Takeishi T, Hirano K, Kobayashi T, Hasegawa G, Hatakeyama K, Naito M. The role of Kupffer cells in liver regeneration. *Arch Histol Cytol* 1999; **62**: 413–422.
  - 17 Kuma S, Inaba M, Ogata H, Inaba K, Okumura T, Saito K *et al*. Effect of human recombinant interleukin-6 on the proliferation of mouse hepatocytes in the primary culture. *Immunobiology* 1990; **180**: 235–242.
  - 18 Satoh M, Yamazaki M. Tumor necrosis factor stimulates DNA synthesis of mouse hepatocytes in primary culture and is suppressed by transforming growth factor beta and interleukin 6. *J Cell Physiol* 1992; **150**: 134–139.
  - 19 Kilkenny C, Browne WJ, Cuthill IC, Emerson M, Altman DG. Improving bioscience research reporting: the ARRIVE guidelines for reporting animal research. *PLoS Biol* 2010; **8**: e1000412.
  - 20 Shi JH, Hammarstrom C, Grzyb K, Line PD. Experimental evaluation of liver regeneration patterns and liver function following ALPPS. *BJS Open* 2017; **1**: 84–96.
  - 21 Shi JH, Scholz H, Huitfeldt HS, Line PD. The effect of hepatic progenitor cells on experimental hepatocellular carcinoma in the regenerating liver. *Scand J Gastroenterol* 2014; **49**: 99–108.
  - 22 Shan B, Wang X, Wu Y, Xu C, Xia Z, Dai J *et al*. The metabolic ER stress sensor IRE1 $\alpha$  suppresses alternative activation of macrophages and impairs energy expenditure in obesity. *Nat Immunol* 2017; **18**: 519–529.
  - 23 Lin Y, Liu L, Jiang H, Zhou J, Tang Y. Inhibition of interleukin-6 function attenuates the central sensitization and pain behavior induced by osteoarthritis. *Eur J Pharmacol* 2017; **811**: 260–267.
  - 24 Badger DA, Kuester RK, Sauer JM, Sipes IG. Gadolinium chloride reduces cytochrome P450: relevance to chemical-induced hepatotoxicity. *Toxicology* 1997; **121**: 143–153.
  - 25 Shi JH, Liu SZ, Wierød L, Scholz H, Anmarkrud JA, Huitfeldt HS *et al*. RAF-targeted therapy for hepatocellular carcinoma in the regenerating liver. *J Surg Oncol* 2013; **107**: 393–401.
  - 26 Garcia-Perez R, Revilla-Nuin B, Martinez CM, Bernabe-Garcia A, Baroja Mazo A, Parrilla Paricio P. Associated liver partition and portal vein ligation (ALPPS) vs selective portal vein ligation (PVL) for staged hepatectomy in a rat model. Similar regenerative response? *PLoS One* 2015; **10**: e0144096.
  - 27 Aldeguer X, Debonera F, Shaked A, Krasinkas AM, Gelman AE, Que X *et al*. Interleukin-6 from intrahepatic cells of bone marrow origin is required for normal murine liver regeneration. *Hepatology* 2002; **35**: 40–48.

- 28 Rai RM, Zhang JX, Clemens MG, Diehl AM. Gadolinium chloride alters the acinar distribution of phagocytosis and balance between pro- and anti-inflammatory cytokines. *Shock* 1996; **6**: 243–247.
- 29 Dong Z, Wei H, Sun R, Tian Z. The roles of innate immune cells in liver injury and regeneration. *Cell Mol Immunol* 2007; **4**: 241–252.
- 30 Tian Y, Jochum W, Georgiev P, Moritz W, Graf R, Clavien PA. Kupffer cell-dependent TNF-alpha signaling mediates injury in the arterialized small-for-size liver transplantation in the mouse. *Proc Natl Acad Sci U S A* 2006; **103**: 4598–4603.
- 31 Kuriyama N, Isaji S, Hamada T, Kishiwada M, Ohsawa I, Usui M *et al.* The cytoprotective effects of addition of activated protein C into preservation solution on small-for-size grafts in rats. *Liver Transpl* 2010; **16**: 1–11.
- 32 Li W, Liang X, Kellendonk C, Poli V, Taub R. STAT3 contributes to the mitogenic response of hepatocytes during liver regeneration. *J Biol Chem* 2002; **277**: 28 411–28 417.

### Supporting information

Additional supporting information can be found online in the Supporting Information section at the end of the article.